

A measurement of the axial form factor of the nucleon by the $p(e, e'\pi^+)n$ reaction at $W = 1125$ MeV

A. Liesenfeld^{a,1}, A. W. Richter^{a,1}, S. Širca^{b,1,2},
 K. I. Blomqvist^a, W. U. Boeglin^a, K. Bohinc^b, R. Böhm^a,
 M. Distler^a, D. Drechsel^a, R. Edelhoff^a, I. Ewald^a,
 J. Friedrich^a, J. M. Friedrich^a, R. Geiges^a, M. Kahrau^a,
 M. Korn^a, K. W. Krygier^a, V. Kunde^a, H. Merkel^a, K. Merle^a,
 U. Müller^a, R. Neuhausen^a, T. Pospischil^a, M. Potokar^b,
 A. Rokavec^b, G. Rosner^a, P. Sauer^a, S. Schardt^a,
 H. Schmieden^a, L. Tiator^a, B. Vodenik^b, A. Wagner^a,
 Th. Walcher^a and S. Wolf^a

^a *Institut für Kernphysik, Universität Mainz, D-55099 Mainz, Germany*

^b *Jožef Stefan Institute, SI-1001 Ljubljana, Slovenia*

The reaction $p(e, e'\pi^+)n$ was measured at the Mainz Microtron MAMI at an invariant mass of $W = 1125$ MeV and four-momentum transfers of $Q^2 = 0.117, 0.195$ and 0.273 (GeV/c)². For each value of Q^2 , a Rosenbluth separation of the transverse and longitudinal cross sections was performed. An effective Lagrangian model was used to extract the ‘axial mass’ from experimental data. We find a value of $M_A = (1.077 \pm 0.039)$ GeV which is (0.051 ± 0.044) GeV larger than the axial mass known from neutrino scattering experiments. This is consistent with recent calculations in chiral perturbation theory.

PACS: 13.60.Le, 25.30.Rw, 14.20.Dh

Keywords: nucleon axial form factor, coincident pion electroproduction

¹ This paper comprises parts of the doctoral theses of A. Liesenfeld, A. W. Richter and S. Širca.

² Corresponding author (tel: +386 61 1773-731, fax: +386 61 219-385, e-mail: simon.sirca@ijs.si).

1 Introduction

There are basically two methods to determine the weak axial form factor of the nucleon. One set of experimental data comes from measurements of (quasi)elastic (anti)neutrino scattering on protons [1], deuterons [2] and other nuclei (Al, Fe) [3,4] or composite targets like freon [5–8] and propane [8,9]. In the (quasi)elastic picture of (anti)neutrino-nucleus scattering, the $\nu N \rightarrow \mu N$ weak transition amplitude can be expressed in terms of the nucleon electromagnetic form factors F_1 and F_2 and the axial form factor G_A . The axial form factor is then extracted by fitting the Q^2 -dependence of the (anti)neutrino-nucleon cross section,

$$\frac{d\sigma}{dQ^2} = A(Q^2) \mp B(Q^2)(s - u) + C(Q^2)(s - u)^2, \quad (1)$$

in which $G_A(Q^2)$ is contained in the bilinear forms $A(Q^2)$, $B(Q^2)$ and $C(Q^2)$ of the relevant form factors and is assumed to be the only unknown quantity. It can be parameterised in terms of an ‘axial mass’ M_A as $G_A(Q^2) = G_A(0)/(1 + Q^2/M_A^2)^2$.

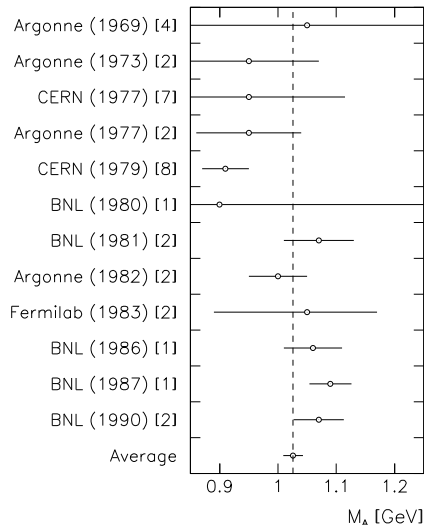


Fig. 1. Axial mass M_A as extracted from (quasi)elastic neutrino and antineutrino scattering experiments. The weighted average is $M_A = (1.026 \pm 0.017)$ GeV, or (1.026 ± 0.021) GeV using the scaled-error averaging recommended by Ref. [10].

Fig. 1 shows the available values for M_A obtained from these studies. References [3,5,6,9] reported severe uncertainties in either knowledge of the incident neutrino flux or reliability of the theoretical input needed to subtract the background from genuine elastic events (both of which gradually improved in subsequent experiments). The values derived fall well outside the most probable range of values known today and exhibit very large statistical and systematic errors. Following the data selection criteria of the Particle Data Group [10], they were excluded from this compilation.

Another body of data comes from charged pion electroproduction on protons [11–17] slightly above the pion production threshold. As opposed to neutrino scattering, which is described by the Cabibbo-mixed $V - A$ theory, the extraction of the axial form factor from electroproduction requires a more involved theoretical picture.

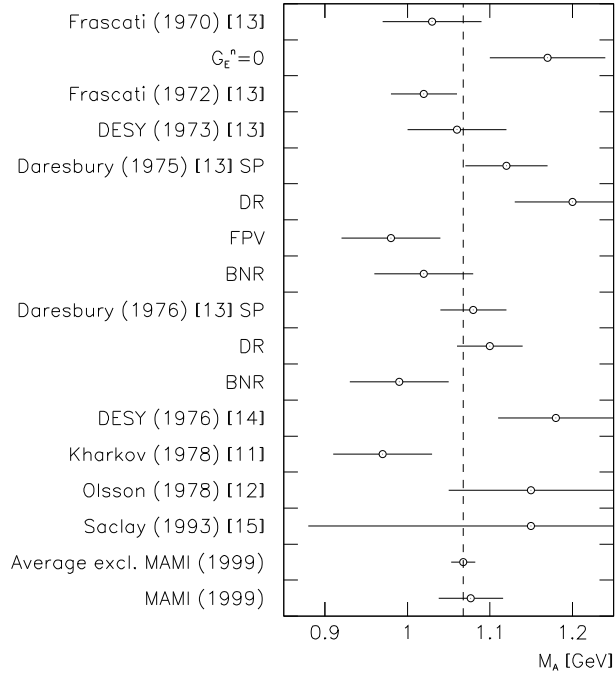


Fig. 2. Axial mass M_A as extracted from charged pion electroproduction experiments. The weighted average (excluding our result) is $M_A = (1.068 \pm 0.015)$ GeV, or (1.068 ± 0.017) GeV using the scaled-error averaging [10]. Including our extracted value, the weighted scaled-error average becomes $M_A = (1.069 \pm 0.016)$ GeV. Note that our value contains both the statistical *and* systematical uncertainty; for other values the systematical errors were not explicitly given. SP: soft-pion limit, DR: analysis using approach of Ref. [21], FPV: Ref. [20], BNR: Ref. [22].

The basic result about low energy photoproduction of massless charged pions can be traced back to the Kroll-Ruderman theorem [18], extended to virtual photons by Nambu, Lurié and Shrauner [19], who obtained the $\mathcal{O}(Q^2)$ result for the isospin $(-)$ (see Ref. [28], p. 29 for notation) electric dipole amplitude at threshold

$$E_{0+}^{(-)}(m_\pi = 0, Q^2) = \frac{eg_A}{8\pi f_\pi} \left\{ 1 - \frac{Q^2}{6} \langle r_A^2 \rangle - \frac{Q^2}{4M^2} \left[\kappa_v + \frac{1}{2} \right] + \mathcal{O}(Q^3) \right\}, \quad (2)$$

where κ_v is the nucleon isovector anomalous magnetic moment, $g_A \equiv G_A(0)$ is the axial coupling constant, and f_π is the pion decay constant.

In the following years, improved models were proposed [16,20–22], most of them including corrections due to the finite pion mass $\mu = m_\pi/M$. The values

of the axial mass were determined, within the framework of the respective model, from the slopes of the angle-integrated differential electroproduction cross sections at threshold,

$$\langle r_A^2 \rangle = -\frac{6}{G_A(0)} \left. \frac{dG_A(Q^2)}{dQ^2} \right|_{Q^2=0} = \frac{12}{M_A^2}. \quad (3)$$

The results of various measurements and theoretical approaches are shown in Fig. 2. Note again that references [16,17] were omitted from the fit for lack of reasonable compatibility with the other results.

Although the results of these investigations deviate from each other by more than their claimed accuracy, the weighted averages from neutrino scattering and electroproduction give quite precise values of the axial mass. Comparing the average values of the two methods, one observes a significant difference of $\Delta M_A = (0.042 \pm 0.023)$ GeV, or (0.042 ± 0.027) GeV using the scaled-error averaging.

Chiral perturbation theory (χ PT) has recently shown a remarkable and model-independent result that already at $\mathcal{O}(Q^2)$, the NLS result of eq. (2) is strongly modified due to pion loop contributions [25]. These contributions effectively reduce the mean-square axial radius,

$$\langle r_A^2 \rangle \rightarrow \langle r_A^2 \rangle + \frac{3}{64f_\pi^2} \left(1 - \frac{12}{\pi^2} \right). \quad (4)$$

The loop correction in eq. (4) has a value of -0.046 fm^2 , which is a -10% correction to a typical $\langle r_A^2 \rangle = 0.45 \text{ fm}^2$. Correspondingly, the axial mass $M_A = \sqrt{12}/\langle r_A^2 \rangle^{1/2}$ would appear to be about 5% larger in electroproduction than in neutrino scattering, in agreement with the observed ΔM_A . The aim of the present investigation was to determine M_A from new, high precision pion electroproduction data and thereby help verify whether this discrepancy was genuine. Since both the energy and momentum transfers were too high to allow for a safe extraction of $E_{0+}^{(-)}$, these data were analysed in the framework of an effective Lagrangian model with the electromagnetic nucleon form factors, the electric pion form factor and the axial nucleon form factor at the appropriate vertices [23,24].

2 Kinematics of the experiment

The differential cross sections for π^+ electroproduction on protons were measured at an invariant mass of $W = 1125 \text{ MeV}$ and at four-momentum transfers

of the virtual photon $Q^2 = 0.117, 0.195$ and 0.273 (GeV/c)². For each value of Q^2 , we measured the scattered electron and the outgoing pion in parallel kinematics at three different polarisations of the virtual photon, enabling us to separate the transverse and the longitudinal part of the cross section by the Rosenbluth technique. Table 1 shows the experimental settings.

Table 1

Experimental settings for the $p(e, e'\pi^+)n$ experiment. The angles are measured with respect to the electron beam axis.

Setting (ε)	Q^2 [GeV ² /c ²]	E_e [MeV]	E'_e [MeV]	θ_e [°]	θ_π [°]	p_π [MeV/c]
0.834	0.117	855.11	587.35	-27.93	39.31	188.84
0.500		510.11	242.35	-58.22	28.31	
0.219		405.11	137.36	92.96	-18.41	
0.742	0.195	855.11	545.79	-37.72	38.27	209.62
0.437		585.11	275.89	66.67	-28.03	
0.229		495.11	185.79	93.45	-20.12	
0.648	0.273	855.11	504.55	46.83	-35.82	228.00
0.457		690.11	339.55	65.27	-29.37	
0.259		585.11	234.55	89.60	-21.90	

3 Experimental setup

The measurements were performed at the Institut für Kernphysik at the University of Mainz, using the continuous-wave electron microtron MAMI [26]. The energies of the incoming electron beam ranged from 405 to 855 MeV, and the beam energy spread did not exceed 0.16 MeV. The 15 to 35 μ A electron beam was scattered on a liquid hydrogen target cell ($5 \times 1 \times 1$ cm³ with 10 μ m Havar walls in settings with the photon polarisation parameter $\varepsilon = 0.437, 0.648, 0.457$ and 0.259, and on a 2 cm-diameter cylindrical target cell with 50 μ m Havar walls in all other settings) attached to a high power target cooling system. Forced circulation and a beam wobbling system were used to avoid density fluctuations of the liquid hydrogen. With this system, luminosities of up to $3.2 \cdot 10^{37}$ cm⁻²s⁻¹ (32 MHz/ μ b) were attained.

The scattered electrons and the produced pions were detected in coincidence by the high resolution ($\delta p/p \approx 10^{-4}$) magnetic spectrometers A (SpecA) and B (SpecB) of the A1 Collaboration [27]. In settings with $\varepsilon = 0.834, 0.500$ and 0.742 , electrons were detected with SpecB and pions with SpecA, and vice versa in all other settings. The momentum acceptance $\Delta p/p$ was 20 % and 15 % in SpecA and SpecB, respectively. Heavy-metal collimators (21 msr in SpecA, 5.1 or 5.6 msr in SpecB) were used to minimise angular acceptance uncertainties due to the relatively large target cells.

A trigger detector system consisting of two planes of segmented plastic scintillators and a threshold Čerenkov detector were used in each spectrometer. The coincidence time resolution, taking into account the different times of flight of particles for different trajectory lengths through the spectrometer, was between 1.0 and 2.6 ns FWHM.

In each spectrometer, four vertical drift chambers were used for particle tracking, measurement of momenta and target vertex reconstruction. Back-tracing the particle trajectories from the drift chambers through the magnetic systems, an angular resolution (all FWHM) better than ± 5 mrad (dispersive and non-dispersive angles) and spatial (vertex) resolution better than ± 5 mm (non-dispersive direction, SpecA) and ± 1 mm (SpecB) were achieved on the target. A more detailed description of the apparatus can be found in Ref. [27].

4 Data analysis

In the offline analysis, cuts in the corrected coincidence time spectrum were applied to identify real coincidences and to eliminate the background of accidental coincidences. A cut in the energy deposited in the first scintillator plane in the pion spectrometer was used to discriminate charged pions against protons. The Čerenkov signal was used to identify electrons in the electron spectrometer and to veto against positrons in the pion spectrometer.

The true coincidences were observed in the peak of the accumulated missing mass distribution $(E_{\text{miss}}^2 - |\mathbf{p}_{\text{miss}}|^2)^{1/2} - M_n$, using an event-by-event reconstruction of $(E_{\text{miss}}, \mathbf{p}_{\text{miss}}) = (\omega + M_p - E_\pi, \mathbf{q} - \mathbf{p}_\pi)$.

The cross sections were subsequently corrected for detector and coincidence inefficiencies (between +1.7 % and +3.2 %) and dead-time losses (between +1.4 % and +4.6 %). The detector efficiencies and their uncertainties were measured by the three-detector method, while the coincidence efficiency of the setup and the uncertainty of the dead-time measurement were determined in simultaneous single-arm and coincidence measurements of elastic $p(e, e'p)$, which was also used to check on the acceptance for the extended targets.

The accepted phase space was determined by a Monte Carlo simulation which provided the (event-wise) Lorentz transformation to the CM system and incorporated radiative corrections and ionisation losses of the incoming and scattered electrons and pions. Full track was kept of the particles' trajectories and their lengths in target and detector materials. Since exact energy losses are not known event-wise, we used the most probable energy losses for the subsequent energy loss correction in both simulation and analysis programs, and compared the corresponding missing mass spectra. The uncertainty estimates were based on relative variations of their content in dependence of the cut-off energy along the radiative tail.

The uncertainty of the integrated luminosity originates only in the target density changes due to temperature fluctuations within the target cell, while the electron beam current is virtually exactly known. Finally, a computer simulation was used to determine the correction factors due to the pion decaying in flight from the interaction point to the scintillation detectors, taking into account the muon contamination at the target (correction factors ranging from $\times 2.23$ to $\times 2.89$ in different settings). The systematical errors of the pion decay correction factors were estimated from the statistical fluctuations of the back-traced muon contamination at the target.

5 Results and discussion

In the Born approximation, the coincidence cross section for pion electroproduction can be factorised as [23,28]

$$\frac{d\sigma}{dE'_e d\Omega'_e d\Omega_\pi^*} = \Gamma_v \frac{d\sigma_v}{d\Omega_\pi^*}, \quad (5)$$

where Γ_v is the virtual photon flux and $d\sigma_v/d\Omega_\pi^*$ is the virtual photon cross section in the CM frame of the final πN system. It can be further decomposed into transverse, longitudinal and two interference parts,

$$\frac{d\sigma_v}{d\Omega_\pi^*} = \frac{d\sigma_T}{d\Omega_\pi^*} + \varepsilon_L^* \frac{d\sigma_L}{d\Omega_\pi^*} + \sqrt{2\varepsilon_L^*(1+\varepsilon)} \frac{d\sigma_{LT}}{d\Omega_\pi^*} \cos\phi_\pi + \varepsilon \frac{d\sigma_{TT}}{d\Omega_\pi^*} \cos 2\phi_\pi \quad (6)$$

with the transverse (ε) and longitudinal ($\varepsilon_L^* = Q^2\varepsilon/\omega^{*2}$) polarisations of the virtual photon fixed by the electron kinematics. The measured cross sections are listed in Table 2.

In parallel kinematics ($\theta_\pi^* = \theta_\pi = 0^\circ$) the interference parts vanish due to their $\sin\theta_\pi^*$ and $\sin^2\theta_\pi^*$ dependence. At constant Q^2 , the transverse and the

Table 2

Measured cross sections in the $p(e, e'\pi^+)n$ reaction.

Setting (ε)	$d\sigma/d\Omega_\pi^*$	Stat. error	Syst. error
	$[\mu\text{b}/\text{sr}]$	$[\mu\text{b}/\text{sr}]$	$[\mu\text{b}/\text{sr}]$
0.834	11.14	0.08 (0.7%)	0.41 (3.7%)
0.500	8.40	0.11 (1.3%)	0.31 (3.7%)
0.219	5.96	0.14 (2.3%)	0.19 (3.2%)
0.742	7.48	0.11 (1.5%)	0.18 (2.4%)
0.437	5.36	0.09 (1.7%)	0.10 (1.8%)
0.229	4.55	0.10 (2.1%)	0.07 (1.6%)
0.648	5.03	0.05 (1.1%)	0.08 (1.6%)
0.457	4.19	0.06 (1.3%)	0.08 (1.8%)
0.259	3.46	0.05 (1.4%)	0.07 (1.9%)

longitudinal cross sections can therefore be separated using the Rosenbluth method by varying ε ,

$$\frac{d\sigma_v}{d\Omega_\pi^*} = \frac{d\sigma_T}{d\Omega_\pi^*} + \varepsilon \frac{Q^2}{\omega^{*2}} \frac{d\sigma_L}{d\Omega_\pi^*}. \quad (7)$$

Not only the statistical, but also the ε -correlated systematical uncertainties of the data were considered in our fit, whereas the ε -independent systematical errors were included in the final uncertainty of $d\sigma_T$ and $d\sigma_L$. The results are shown in Fig. 3 and Table 3. The Q^2 -dependence of the separated transverse and longitudinal cross sections can be seen in Fig. 4, together with the theoretical fits used to extract the form factors.

Since values of $\nu = -Q^2/M^2$ and W in this experiment were too high for a direct application of χ PT, an effective Lagrangian model [23,24] was used to analyse the measured Q^2 -dependence of the cross section, and to extract the nucleon axial and pion charge form factors. In the energy region of our experiment, the pseudovector π NN coupling evaluated at tree-level provided an adequate description of the reaction cross section. We included the s - and u -channel nucleon pole terms containing electric and magnetic Sachs nucleon form factors of the well-known dipole form with a ‘cut-off’ $\Lambda_d = 0.843$ GeV, the t -channel pion pole term with a monopole form factor $F_\pi(Q^2) = 1/(1 + Q^2/\Lambda_\pi^2)$, the contact (seagull) term with the axial dipole form factor

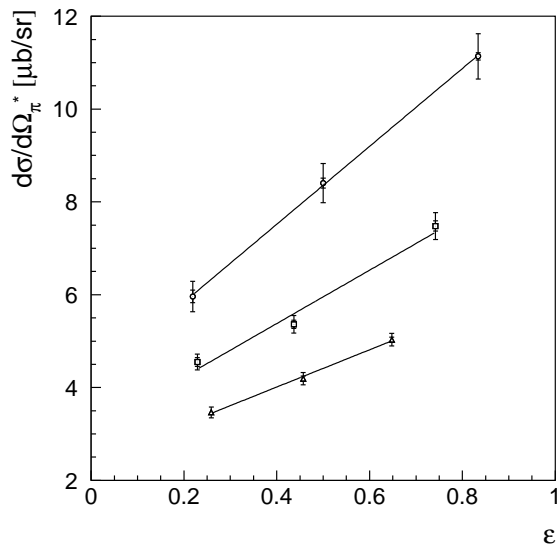


Fig. 3. Least-squares straight-line fits to the measured cross sections for $p(e, e'\pi^+)n$ at $W = 1125$ MeV, for three values of Q^2 . The smaller error bars correspond to statistical, the larger ones to the sum of statistical and systematical errors.

Table 3

The results of the L/T separation based on the least-squares fit to the data.

Setting (Q^2) [GeV ² /c ²]	$d\sigma_T/d\Omega_\pi^*$ [μb/sr]	$(Q^2/\omega^{*2}) d\sigma_L/d\Omega_\pi^*$ [μb/sr]
0.117	$4.160 \pm 0.165_{\text{stat}} \pm 0.202_{\text{sys}}$	$8.394 \pm 0.254_{\text{stat}} \pm 0.481_{\text{sys}}$
0.195	$3.080 \pm 0.139_{\text{stat}} \pm 0.051_{\text{sys}}$	$5.747 \pm 0.284_{\text{stat}} \pm 0.246_{\text{sys}}$
0.273	$2.406 \pm 0.088_{\text{stat}} \pm 0.056_{\text{sys}}$	$4.012 \pm 0.187_{\text{stat}} \pm 0.052_{\text{sys}}$

$G_A(Q^2) = G_A(0)/(1 + Q^2/M_A^2)^2$, and the s -channel Δ -resonance term. Vector meson exchange contributions in the t -channel were found to play a negligible role in the charged pion channel.

Due to cancellations between higher partial waves and interference terms with the s -wave, $d\sigma_T$ is predominantly sensitive to the $E_{0+}(n\pi^+)$ amplitude and therefore to M_A . On the other hand, the pion charge form factor appears in the longitudinal amplitude $L_{0+}(n\pi^+)$ only at order $\mathcal{O}(\mu^2, \mu\nu)$, and the s -wave contribution to $d\sigma_L$ amounts to 10% only. Due to the contributions of the higher partial waves, however, the longitudinal cross section $d\sigma_L$ is quite sensitive to Λ_π , which is a bonus ‘by-product’ of the analysis.

Since current conservation is violated if arbitrary form factors are included, gauge invariance was imposed by additional gauge terms in the hadronic cur-

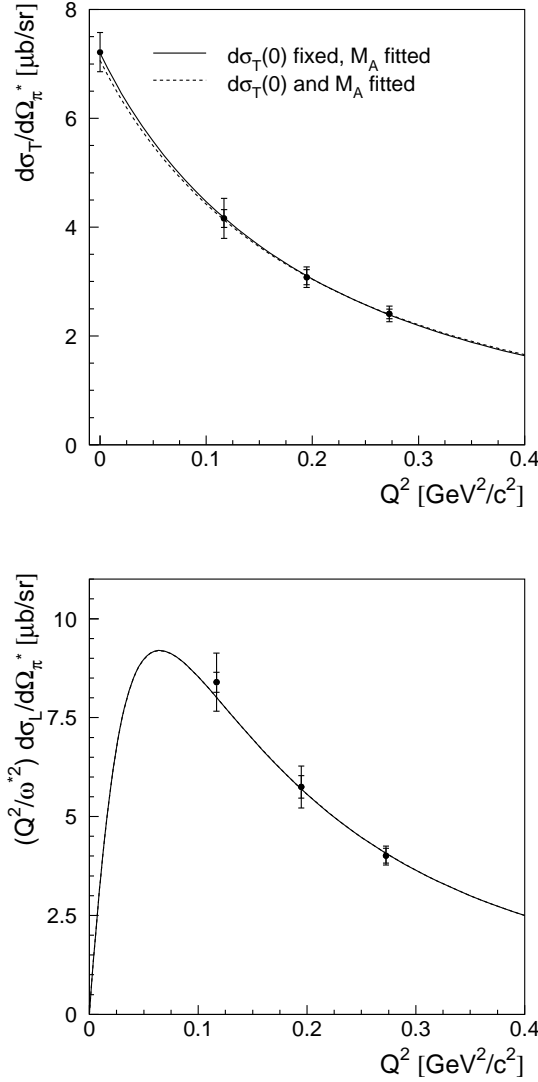


Fig. 4. Separated transverse and longitudinal cross sections. The solid line shows our fit with $d\sigma_T/d\Omega_\pi^*(Q^2 = 0)$ fixed to $(7.22 \pm 0.36) \mu\text{b/sr}$; the dotted line is the unconstrained fit. In the longitudinal part the fits are almost indistinguishable. The smaller error bars correspond to statistical, the larger ones to the sum of statistical and systematical errors.

rent. These terms modify the longitudinal part of the cross section and therefore influence the pion pole term and thus the extracted value of Λ_π . However, this procedure does not affect the transverse part of the cross section. The axial mass can then be determined from the Q^2 -dependence of $d\sigma_T$, and the result can be compared to the prediction of χPT . In the theoretical fit, the transverse part is fitted first.

We have used two different techniques to determine the axial mass:

(I) Only the axial mass was varied, whereas the value of $d\sigma_T$ at $Q^2 = 0$ was fixed by extrapolating the transverse cross section (i. e. the $E_{0+}(n\pi^+)$ amplitude) to the value of the photoproduction angular distribution at $\theta_\pi = 0^\circ$. A precise cross section at the photon point ($Q^2 = 0$) is very helpful for our analysis and can reduce the uncertainty in determining the axial mass considerably. Unfortunately, there are no experimental data available around $W = 1125$ MeV and forward angles. The only measurements in this energy region are performed at pion angles larger than 60° with large deviations among the different data sets. Therefore we have used a value at the photon point obtained from different partial-wave analyses of the VPI group [29] and of the Mainz dispersion analysis [30]. This yields to a weighted-average cross section at the photon point of $(7.22 \pm 0.36) \mu\text{b}/\text{sr}$ and this value was used as an additional data point. The corresponding value of $E_{0+}(n\pi^+)$ is also well supported by the studies of the GDH sum rule [31] and by the low energy theorem (Kroll-Ruderman limit).

(II) The three data points alone were fitted, while the value of the transverse cross section at $Q^2 = 0$ was taken as an additional parameter, with the result $d\sigma_T(0) = (7.06 \pm 1.12) \mu\text{b}/\text{sr}$.

The best-fit parameters for the transverse cross section were then used to fit the longitudinal part.

Using the first and preferred procedure, we find from the transverse cross section $M_A = (1.077 \pm 0.039)$ GeV, corresponding to $\langle r_A^2 \rangle^{1/2} = (0.635 \pm 0.023)$ fm. From the longitudinal part, we obtain $\Lambda_\pi = (0.654 \pm 0.027)$ GeV, corresponding to $\langle r_\pi^2 \rangle^{1/2} = (0.740 \pm 0.031)$ fm. The second procedure leads to the following results: $M_A = (1.089 \pm 0.106)$ GeV or $\langle r_A^2 \rangle^{1/2} = (0.628 \pm 0.061)$ fm, and $\Lambda_\pi = (0.658 \pm 0.028)$ GeV or $\langle r_\pi^2 \rangle^{1/2} = (0.734 \pm 0.031)$ fm.

6 Summary and conclusions

We have measured the electroproduction of positive pions on protons at the invariant mass of $W = 1125$ MeV, and at four-momentum transfers of $Q^2 = 0.195 (\text{GeV}/c)^2$ and $0.273 (\text{GeV}/c)^2$. In conjunction with our previous measurement at $Q^2 = 0.117 (\text{GeV}/c)^2$ [23], we were then able to study the Q^2 -dependence of the transverse and longitudinal cross sections, separated by the Rosenbluth technique for each Q^2 . The statistical uncertainties were between 0.7% and 2.3%, an improvement of an order of magnitude over the result of Ref. [33]. The systematical uncertainties were estimated to be between 1.6% and 3.7%, and are expected to decrease significantly in the future experiments.

We have extracted the axial mass parameter M_A of the nucleon axial form factor from our pion electroproduction data using an effective Lagrangian model with pseudovector πNN coupling. Our extracted value of $M_A = (1.077 \pm 0.039)$ GeV is (0.051 ± 0.044) GeV larger than the axial mass $M_A = (1.026 \pm 0.021)$ GeV known from neutrino scattering experiments. Our result essentially confirms with the scaled-error weighted average $M_A = (1.068 \pm 0.017)$ GeV of older pion electroproduction experiments. If we include our value into the database, the weighted average increases to $M_A = (1.069 \pm 0.016)$ GeV, and the ‘axial mass discrepancy’ becomes $\Delta M_A = (0.043 \pm 0.026)$ GeV. This value of ΔM_A is in agreement with the prediction derived from χ Pt, $\Delta M_A = 0.056$ GeV. We conclude that the puzzle of seemingly different axial radii as extracted from pion electroproduction and neutrino scattering can be resolved by pion loop corrections to the former process, and that the size of the predicted corrections is confirmed by our experiment.

Theoretical input needed to extract the axial mass and the pion radius has naturally led to some model dependence of the results. The dominant contribution to pion electroproduction at $W = 1125$ MeV is due to the Born terms. These are based on very fundamental grounds and the couplings are very well known. For our purpose the electric and magnetic form factors of the nucleons are also accurately known whereas the remaining two (the axial and the pion form factors) are the subjects of our analysis. In parallel kinematics we are in the ideal situation where the pion form factor contributes only to the longitudinal cross section, therefore reducing very strongly the model dependence of the transverse cross section and consequently of the determination of the axial mass. Furthermore, the Δ resonance, which plays the second important role in our theoretical description, also contributes with a well-known M1 excitation to the transverse cross section, while the longitudinal C2 excitation gives rise to a larger uncertainty due to the less known C2 form factor, currently under investigation at different laboratories.

Altogether, the model dependence is smaller for extracting the axial mass than for the pion radius. This could partly explain the discrepancy in the different values of the pion radius between our analysis and the analysis of pion scattering off atomic electrons [32]. However, as in the case of the axial mass, an additional correction of the pion radius obtained from electroproduction experiments is very likely. This should be investigated in future studies of chiral perturbation theory.

Acknowledgement

This work was supported by the Deutsche Forschungsgemeinschaft, SFB 201.

References

- [1] G. Fanourakis et al., Phys. Rev. D **21** (1980) 562;
L. A. Ahrens et al., Phys. Rev. D **35** (1987) 785;
L. A. Ahrens et al., Phys. Lett. B **202** (1988) 284.
- [2] S. J. Barish et al., Phys. Rev. D **16** (1977) 3103;
K. L. Miller et al., Phys. Rev. D **26** (1982) 537;
W. A. Mann et al., Phys. Rev. Lett. **31** (1973) 844;
N. J. Baker et al., Phys. Rev. D **23** (1981) 2499;
T. Kitagaki et al., Phys. Rev. D **28** (1983) 436;
T. Kitagaki et al., Phys. Rev. D **42** (1990) 1331.
- [3] M. Holder et al., Nuovo Cim. A **LVII** (1968) 338.
- [4] R. L. Kustom et al., Phys. Rev. Lett. **22** (1969) 1014.
- [5] D. Perkins, in: *Proceedings of the 16th International Conference on High Energy Physics*, J. D. Jackson, A. Roberts (eds.), National Accelerator Laboratory, Batavia, Illinois, 1973, Vol. IV, 189.
- [6] A. Orkin-Lecourtois and C. A. Piketty, Nuovo Cim. A **L** (1967) 927.
- [7] S. Bonetti et al., Nuovo Cim. A **38** (1977) 260.
- [8] N. Armenise et al., Nucl. Phys. B **152** (1979) 365.
- [9] I. Budagov et al., Lett. Nuovo Cim. **II** (1969) 689.
- [10] C. Caso et al. (Particle Data Group), *Review of Particle Properties*, Eur. Phys. J. C **3** (1998) 9.
- [11] A. S. Esaulov, A. M. Pilipenko, Yu. I. Titov, Nucl. Phys. B **136** (1978) 511.
- [12] M. G. Olsson, E. T. Osypowski and E. H. Monsay, Phys. Rev. D **17** (1978) 2938.
- [13] E. Amaldi et al., Nuovo Cim. A **LXV** (1970) 377;
E. Amaldi et al., Phys. Lett. B **41** (1972) 216;
P. Brauel et al., Phys. Lett. B **45** (1973) 389;
A. del Guerra et al., Nucl. Phys. B **99** (1975) 253;
A. del Guerra et al., Nucl. Phys. B **107** (1976) 65.
- [14] P. Joos et al., Phys. Lett. B **62** (1976) 230.
- [15] S. Choi et al., Phys. Rev. Lett. **71** (1993) 3927.
- [16] Y. Nambu and M. Yoshimura, Phys. Rev. Lett. **24** (1970) 25.
- [17] E. D. Bloom et al., Phys. Rev. Lett. **30** (1973) 1186.
- [18] N. M. Kroll and M. A. Ruderman, Phys. Rev. **93** (1954) 233.

- [19] Y. Nambu and D. Lurié, Phys. Rev. **125** (1962) 1429;
Y. Nambu and E. Shrauner, Phys. Rev. **128** (1962) 862.
- [20] G. Furlan, N. Paver and C. Verzegnassi, Nuovo Cim. A **LXX** (1970) 247;
C. Verzegnassi, Springer Tracts in Modern Physics **59** (1971) 154;
G. Furlan, N. Paver and C. Verzegnassi, Springer Tracts in Modern Physics
62 (1972) 118.
- [21] N. Dombey and B. J. Read, Nucl. Phys. B **60** (1973) 65;
B. J. Read, Nucl. Phys. B **74** (1974) 482.
- [22] G. Benfatto, F. Nicolò and G. C. Rossi, Nucl. Phys. B **50** (1972) 205;
G. Benfatto, F. Nicolò and G. C. Rossi, Nuovo Cim. A **14** (1973) 425.
- [23] K. I. Blomqvist et al. (A1 Collaboration), Z. Phys. A **353** (1996) 415.
- [24] D. Drechsel and L. Tiator, J. Phys. G: Nucl. Part. Phys. **18** (1992) 449.
- [25] V. Bernard, N. Kaiser and U.-G. Meißner, Phys. Rev. Lett. **69** (1992) 1877;
V. Bernard, N. Kaiser and U.-G. Meißner, Phys. Rev. Lett. **72** (1994) 2810.
- [26] H. Herminghaus et al., Proc. LINAC Conf. 1990, Albuquerque, New Mexico;
J. Ahrens et al., Nucl. Phys. News **2** (1994) 5.
- [27] K. I. Blomqvist et al., Nucl. Instr. Meth. A **403** (1998) 263.
- [28] E. Amaldi, S. Fubini and G. Furlan, Springer Tracts in Modern Physics **83**
(1979) 6.
- [29] R. A. Arndt, I. I. Strakovsky and R. L. Workman, Phys. Rev. C **53** (1996) 430;
see also the web-page <http://said.phys.vt.edu/analysis/go3pr.html>.
- [30] O. Hanstein, D. Drechsel, L. Tiator, Nucl. Phys. A **632** (1998) 561.
- [31] D. Drechsel and G. Krein, Phys. Rev. D **58** (1998) 116009.
- [32] S. R. Amendolia et al., Phys. Lett. B **146** (1984) 116;
S. R. Amendolia et al., Phys. Lett. B **178** (1986) 435.
- [33] G. Bardin et al., Nucl. Phys. B **120** (1977) 45.